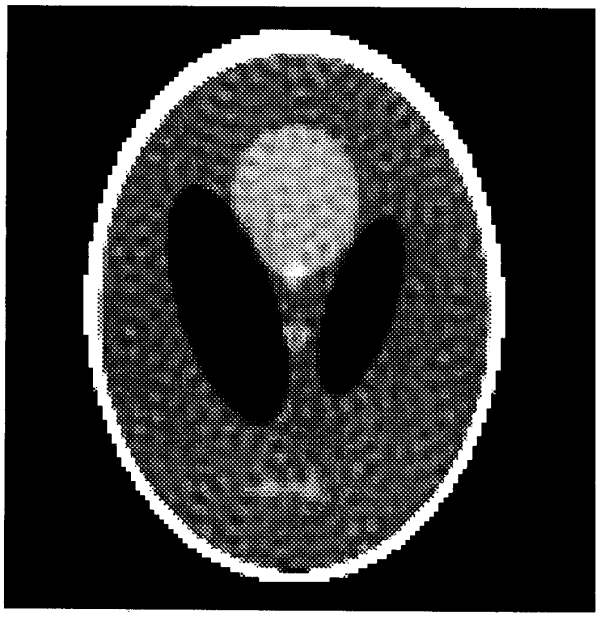

Fig. 10. The noisy image for Example 4, obtained from the noisy projections of the Shepp-Logan phantom.

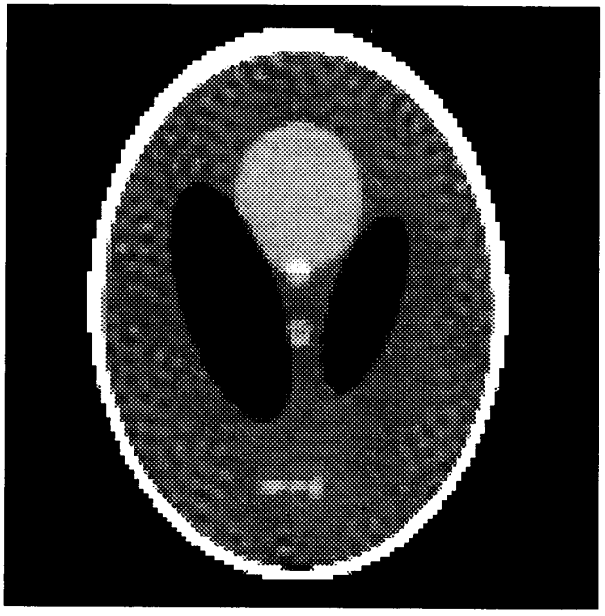

Fig. 11. MMSE image obtained by constraining the wavelet coefficients of the noisy image; Example 4.

threshold is used to set the finest-scale coefficients to zero. The resulting MMSE image is shown in Fig. 11. The noise power has been reduced by 20.3% in the whole image, while still preserving the edges.

References

[1] S. R. Deans, *The Radon Transform and Some of its Applications*. New York: Wiley, 1983.

[2] S. Mallat, "A theory for multiresolution signal decomposition: The wavelet representation," *IEEE Trans. Patt. Anal. Machine Intell.*, vol. PAMI-11, pp. 674–693, 1989.

[3] I. Daubechies, "Orthonormal bases of compactly supported wavelets," *IEEE Trans. Inform. Theory*, vol. 36, pp. 961–1005, 1990.

[4] B. E. A. Saleh and N. S. Subotic, "Time-variant filtering of signals in the mixed time-frequency domain," *IEEE Trans. Acoust., Speech, Signal Processing*, vol. ASSP-33, pp. 1479–1487, 1985.

[5] T. E. Koczwara and D. L. Jones, "On mask selection for time-varying filtering using the Wigner distribution," in *Proc. ICASSP*, Albuquerque, NM, 1990, pp. 2487–2490.

[6] M. Bikdash and K. B. Yor, "Linear shift varying filtering of nonstationary chirp signals," in *Proc. ICASSP*, New York, 1988, pp. 428–432.

[7] B. Boashash and L. B. White, "Instantaneous frequency estimation and automatic time-varying filtering," in *Proc. ICASSP*, Albuquerque, NM, 1990, pp. 1221–1224.

[8] J. Jeong and W. J. Williams, "Time-varying filtering and signal synthesis," in *Time-Frequency Signal Analysis*, B. Boashash, Ed. Melbourne: Longman and Cheshire, 1991.

[9] G. F. Boudreaux-Bartels and T. W. Parks, "Time-varying filtering and signal estimation using Wigner distribution synthesis techniques," *IEEE Trans. Acoust., Speech, Signal Processing*, vol. 34, pp. 442–451, 1988.

[10] H. L. Van Trees, *Detection, Estimation, and Modulation Theory*. New York: Wiley, 1968.

[11] A. K. Jain and S. Ansari, "Radon transform theory for random fields and optimum image reconstruction from noisy projections," in *Proc. ICASSP*, San Diego, CA, 1984, pp. 12A.7.1–12A.7.4.

[12] L. A. Shepp and B. F. Logan, "The Fourier reconstruction of a head section," *IEEE Trans. Nucl. Sci.*, vol. NS-21, pp. 21–42, 1974.

Multiresolution Representations Using the Auto-Correlation Functions of Compactly Supported Wavelets

Naoki Saito and Gregory Beylkin

Abstract—**We propose a shift-invariant multiresolution representation of signals or images using dilations and translations of the auto-correlation functions of compactly supported wavelets. Although these functions do not form an orthonormal basis, their properties make them useful for signal and image analysis. Unlike wavelet-based orthonormal representations, our representation has 1) symmetric analyzing functions, 2) shift-invariance, 3) associated iterative interpolation schemes, and 4) a simple algorithm for finding the locations of the multiscale edges as zero-crossings.**

We also develop a noniterative method for reconstructing signals from their zero-crossings (and slopes at these zero-crossings) in our representation. This method reduces the reconstruction problem to that of solving a system of linear algebraic equations.

Manuscript received February 3, 1992; revised June 3, 1993. The Guest Editor coordinating the review of this paper and approving it for publication was Prof. Martin Vetterli.

N. Saito is with Schlumberger-Doll Research, Ridgefield, CT 06877 and the Department of Mathematics, Yale University, New Haven, CT 06250.

G. Beylkin is with the Program in Applied Mathematics, University of Colorado at Boulder, Boulder, CO 80309-0526.

IEEE Log Number 9212194.

I. Introduction

By analyzing the growth or decay from scale to scale of the coefficients of the orthonormal wavelet expansions, it is possible to estimate the local behavior of signals. However, since the coefficients of the orthonormal wavelet expansions are not shift-invariant, redundant representations (without subsampling at each scale, e.g., [3], [20]–[22], or the continuous wavelet transforms [13]) are being used in order to simplify the analysis of coefficients from scale to scale. In particular, the orthonormal wavelet expansion of a vector of length N without subsampling is not only shift-invariant but also contains all the wavelet coefficients to represent N circularly-shifted versions of the original signal [2], [21], [22].

The asymmetric shape of the orthonormal compactly supported wavelets presents another difficulty for the analysis of signals. The symmetric basis functions are preferred since, for example, their use simplifies finding zero-crossings (or extrema) corresponding to the locations of edges in images at later stages of processing. There are several approaches for dealing with this problem. The first approach consists in constructing approximately symmetric orthonormal wavelets and gives rise to approximate quadrature mirror filters [14]. The second consists in using biorthogonal bases [4], [23], so that the basis functions may be chosen to be exactly symmetric.

Alternatively, a redundant (shift-invariant) representation using dilations and translations of the auto-correlation functions of compactly supported wavelets (*the auto-correlation shell*), may be used for signal analysis instead of the wavelets per se. The exact filters for the decomposition are the auto-correlations of the quadrature mirror filter coefficients of the compactly supported wavelets and, therefore, are exactly symmetric. The recursive definition of the auto-correlation functions of compactly supported wavelets leads to fast iterative algorithms to generate the shift-invariant multiresolution representations.

One of the interesting features of this representation is its convertibility to the redundant expansion (without subsampling) by the corresponding orthonormal wavelets on each scale, independently of other scales. An algorithm for this conversion is discussed in detail in [21].

As an application of the proposed representation, we will also consider the reconstruction of signals from zero-crossings (and slopes at zero-crossings), i.e., the conversion of the auto-correlation shell representation into the zero-crossing-based representation. Such a representation is useful for nonlinear manipulation of signals; for example, edge-preserving smoothing and interpolation (see [15], [16], [18], [19]).

There is also a simple relation between the auto-correlation shell representation and the continuous wavelet transform [13] which will be reported elsewhere.

II. Wavelets and their Auto-correlation Functions

The auto-correlation functions of compactly supported scaling functions were first studied (as the so-called fundamental functions) in the context of the Lagrange iterative interpolation scheme by Dubuc [10] and Deslauriers and Dubuc [9] before compactly supported wavelets were developed in [7]. Later, applications of the auto-correlation functions of compactly supported scaling functions and wavelets for signal representation and analysis were developed by Ansari *et al.* [1] and Shensa [22], and, independently, in [21].

Let $\Phi(x)$ be the auto-correlation function,

$$\Phi(x) = \int_{-\infty}^{+\infty} \varphi(y)\, \varphi(y - x)\, dy, \tag{2.1}$$

where $\varphi(x)$ is the scaling function which appears in the construction of compactly supported wavelets in [7]. The function $\Phi(x)$ is exactly the "fundamental function" of the symmetric iterative interpolation scheme introduced in [9], [10]. Thus, there is a simple one-to-one correspondence between iterative interpolation schemes and compactly supported wavelets [1], [21], [22]. In particular, the scaling function corresponding to Daubechies's wavelet with two vanishing moments yields the scheme in [10]. In general, the scaling function corresponding to Daubechies's wavelet with M vanishing moments leads to an iterative interpolation scheme which uses the Lagrange polynomial of degree $2M - 1$ [9]. Additional variants of iterative interpolation schemes may be obtained using the compactly supported scaling functions (e.g., "coiflets") described in [8].

Let us outline the derivation of the two-scale difference equation for the function $\Phi(x)$. Let $m_0(\xi)$ and $m_1(\xi)$ be the 2π-periodic functions,

$$m_0(\xi) = \frac{1}{\sqrt{2}} \sum_{k=0}^{L-1} h_k e^{ik\xi},$$

$$m_1(\xi) = \frac{1}{\sqrt{2}} \sum_{k=0}^{L-1} g_k e^{ik\xi} = e^{i(\xi+\pi)} \overline{m_0(\xi + \pi)} \tag{2.2}$$

satisfying the quadrature mirror (filter) condition,

$$|m_0(\xi)|^2 + |m_1(\xi)|^2 = 1. \tag{2.3}$$

If we consider trigonometric polynomial solutions of (2.3), then from (2.2) and (2.3) it follows that

$$|m_0(\xi)|^2 = \frac{1}{2} + \frac{1}{2} \sum_{k=1}^{L/2} a_{2k-1} \cos(2k - 1)\xi \tag{2.4}$$

where $\{a_k\}$ are the auto-correlation coefficients of the filter $H = \{h_k\}_{0 \le k \le L-1}$,

$$a_k = 2 \sum_{l=0}^{L-1-k} h_l h_{l+k}, \qquad k = 1, \cdots, L - 1,$$

and

$$a_{2k} = 0, \qquad k = 1, \cdots, L/2 - 1. \tag{2.5}$$

Using the two-scale difference equation for the scaling function φ,

$$\varphi(x) = \sqrt{2} \sum_{k=0}^{L-1} h_k \varphi(2x - k) \tag{2.6}$$

it is easy to verify that

$$\Phi(x) = \Phi(2x) + \frac{1}{2} \sum_{l=1}^{L/2} a_{2l-1} (\Phi(2x - 2l + 1) + \Phi(2x + 2l - 1)). \tag{2.7}$$

Introducing the auto-correlation function of the wavelet ψ,

$$\Psi(x) = \int_{-\infty}^{+\infty} \psi(y) \psi(y - x)\, dy \tag{2.8}$$

where

$$\psi(x) = \sqrt{2} \sum_{k=0}^{L-1} g_k \varphi(2x - k) \tag{2.9}$$

we also have

$$\Psi(x) = \Phi(2x) - \frac{1}{2} \sum_{l=1}^{L/2} a_{2l-1} (\Phi(2x - 2l + 1) + \Phi(2x + 2l - 1)). \tag{2.10}$$

By direct examination of (2.7) and (2.10), we find that both Φ and Ψ are supported within the interval $[-L+1, L-1]$.

Finally, $\Phi(x)$ and $\Psi(x)$ have vanishing moments,

$$\mathfrak{M}_{\Psi}^{m} = \int_{-\infty}^{+\infty} x^{m}\Psi(x)\,dx = 0 \qquad \text{for } 0 \le m \le L, \tag{2.11}$$

$$\mathfrak{M}_{\Phi}^{m} = \int_{-\infty}^{+\infty} x^{m}\Phi(x)\,dx = 0 \qquad \text{for } 1 \le m \le L \tag{2.12}$$

and

$$\int_{-\infty}^{+\infty} \Phi(x)\,dx = 1. \tag{2.13}$$

It is easy to verify (see [2]) that even moments of the coefficients a_{2k-1} from (2.5) vanish, namely

$$\sum_{k=1}^{L/2} a_{2k-1}(2k-1)^{2m} = 0 \qquad \text{for } 1 \le m \le M-1 \tag{2.14}$$

where $M = L/2$ (for wavelets in [7]). Since L consecutive moments of the auto-correlation function $\Psi(x)$ vanish (2.11), we have for small $|\xi|$

$$\hat{\Psi}(\xi) = O(\xi^{L}) \tag{2.15}$$

where $\hat{\Psi}(\xi)$ is the Fourier transform of $\Psi(x)$. Thus, $\hat{\Psi}(\xi)$ may be viewed as the symbol of a pseudo-differential operator which behaves like an approximation of the derivative operator $(d/dx)^{L}$. Therefore, the operator of convolution with $\Psi(x)$ behaves essentially like a differential operator in detecting changes of spatial intensity. We display functions $\Phi(x)$, $\varphi(x)$, $\Psi(x)$, $\psi(x)$, and the magnitudes of their Fourier transforms in Figs. 1 and 2.

Let us briefly review the relation of the auto-correlation functions in (2.1) and (2.8) to the iterative interpolation scheme. Let B_n be the set of dyadic rationals $m/2^n$, $m \in \mathbf{Z}$ and $n = 0, 1, 2, \cdots$. Following [9] and [10], let us consider the following problem: given values of $f(x)$ on B_0, extend f to B_1, B_2, $\cdots$ in an iterative manner. For $x \in B_{n+1} \backslash B_n$, Dubuc [10] suggested the following formula to compute the value $f(x)$,

$$f(x) = \frac{9}{16}\left(f(x-h) + f(x+h)\right) - \frac{1}{16}\left(f(x-3h) + f(x+3h)\right) \tag{2.16}$$

where $h = 1/2^{n+1}$. We illustrate a few steps of this iterative process applied to the unit impulse in Fig. 3.

This interpolation scheme is generalized further in [9],

$$f(x) = \sum_{k \in Z} F(k/2) f(x + kh) \qquad \text{for } x \in B_{n+1} \backslash B_n \tag{2.17}$$

where $h = 1/2^{n+1}$, and the coefficients $F(k/2)$ are computed by generating the function satisfying

$$F(x/2) = \sum_{k \in Z} F(k/2) F(x-k). \tag{2.18}$$

Using the Lagrange polynomials with $L = 2M$ nodes, we have

$$f(x) = \sum_{k=1}^{M} \mathcal{P}_{2k-1}^{L-1}(0)\left(f(x-(2k-1)h) + f(x+(2k-1)h)\right) \tag{2.19}$$

where $\{\mathcal{P}_{2k-1}^{L-1}(x)\}_{-M+1 \le k \le M}$ is a set of Lagrange polynomials of the degree $L-1$ with nodes $\{-L+1, -L+3, \cdots, L-3, L-1\}$, i.e.,

$$\mathcal{P}_{2k-1}^{L-1}(x) = \prod_{l=-M+1, l \ne k}^{M} \frac{x-(2l-1)}{(2k-1)-(2l-1)}. \tag{2.20}$$

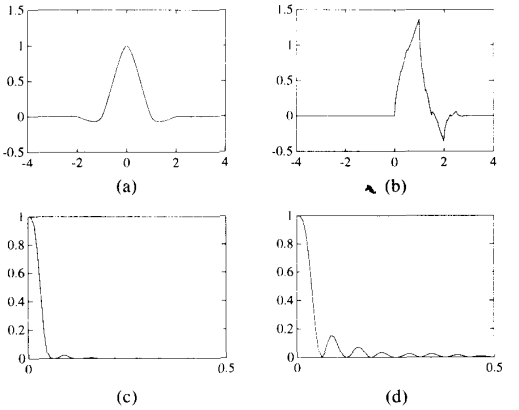

Fig. 1. Plots of the auto-correlation function $\Phi(x)$ and Daubechies's scaling function $\varphi(x)$ with $L = 2M = 4$. (a) $\Phi(x)$. (b) $\varphi(x)$. (c) Magnitude of the Fourier transform of $\Phi(x)$. (d) Magnitude of the Fourier transform of $\varphi(x)$.

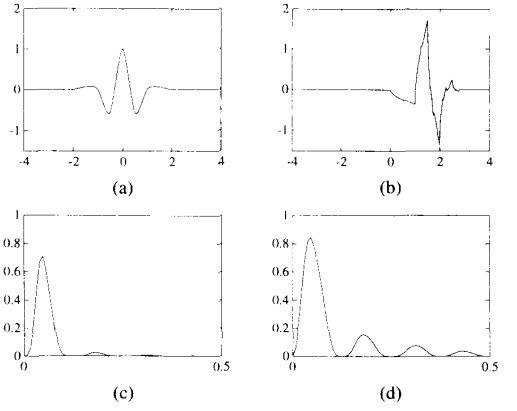

Fig. 2. Plots of the auto-correlation function $\Psi(x)$ and Daubechies's wavelet $\psi(x)$ with $L = 2M = 4$. (a) $\Psi(x)$. (b) $\psi(x)$. (c) Magnitude of the Fourier transform of $\Psi(x)$. (d) Magnitude of the Fourier transform of $\psi(x)$.

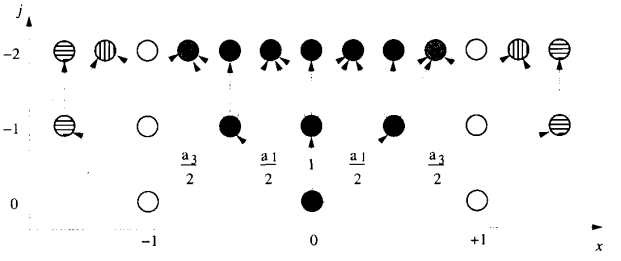

Fig. 3. The Lagrange iterative interpolation of the unit impulse sequence with the associated quadrature mirror filter of length $L = 4$, i.e., $a_1 = 9/8$ and $a_3 = -1/8$. Black nodes at $x = 0$ indicate 1 and white nodes at $x = \pm 1$ have value 0. Shaded nodes have values other than 0 or 1. Note that the values of nodes existing at the jth scale do not change at the $(j-1)$-th scale and higher. The result of repeating this procedure converges to $\Phi(x)$ as $j \to -\infty$.

In this case, (2.18) reduces to

$$F(x) = F(2x) + \sum_{k=1}^{M} \mathcal{O}_{2k-1}^{L-1}(0)(F(2x - 2k + 1) + F(2x + 2k - 1)). \quad (2.21)$$

This special case of (2.17) is called the "Lagrange iterative interpolation." The original scheme (2.16) of Dubuc corresponds to $L = 4$ in (2.19).

We have

$$F(x) = \Phi(x), \quad (2.22)$$

where $F(x)$ is the fundamental function defined in (2.18) and $\Phi(x)$ is the auto-correlation function of the scaling function $\varphi(x)$. Using the two-scale difference equation (2.7), we obtain

$$\Phi(k/2) = \Phi(k) + \frac{1}{2}\sum_{l\in N} a_{2l-1}(\Phi(k - 2l + 1) + \Phi(k + 2l - 1)), \quad (2.23)$$

and, therefore,

$$\Phi(k/2) = a_k/2. \quad (2.24)$$

In other words, the two-scale difference equation for the function Φ in (2.7) may be rewritten as

$$\Phi(x/2) = \sum_{k\in Z} \Phi(k/2)\Phi(x - k). \quad (2.25)$$

For any polynomial P of degree smaller than L, the Lagrange iterative interpolation of the sequence $f(n) = P(n)$, $n \in \mathbf{Z}$, via (2.19) is precisely the function $f(x) = P(x)$ for any $x \in \mathbf{R}$.

If the number of vanishing moments $M = 1$ and $L = 2$ (the Haar basis), then we have

$$\Phi_{\text{Haar}}(x) = \begin{cases} 1 + x & \text{for } -1 \le x \le 0, \\ 1 - x & \text{for } 0 \le x \le 1, \\ 0 & \text{otherwise} \end{cases} \quad (2.26)$$

and the interpolation process corresponds to linear interpolation.

Using expressions (3.49)–(3.52) of [2], the relation (2.4) may be rewritten as

$$|m_0(\xi)|^2 = \frac{1}{2} + \frac{1}{2}\left[\frac{(2M-1)!}{(M-1)!\,4^{M-1}}\right]^2 \cdot \sum_{k=1}^{M} \frac{(-1)^{k-1}\cos(2k-1)\xi}{(2k-1)(M-k)!(M+k-1)!}. \quad (2.27)$$

If $M \to \infty$, then

$$|m_0(\xi)|^2 \to \frac{1}{2} + \frac{2}{\pi}\sum_{k=1}^{\infty} \frac{(-1)^{k-1}}{2k-1}\cos(2k-1)\xi \quad (2.28)$$

which is the Fourier series of the characteristic function of $[-\pi/2, \pi/2]$. This implies that the corresponding auto-correlation function is

$$\Phi_\infty(x) = \text{sinc}(x) = \frac{\sin \pi x}{\pi x}, \quad (2.29)$$

and the interpolation process corresponds to band-limited interpolation. (It turns out that in this case the scaling function coincides with its auto-correlation function.) Thus, we have a family of symmetric iterative interpolation schemes parameterized by the number of vanishing moments $1 \le M < \infty$.

In what follows, we will need to compute the derivatives of the auto-correlation functions in (2.1) and (2.8). Note that the derivative of the function $f(x)$ in (2.19) is computed via

$$f'(x) = \sum_{k=1}^{L-1} r_k(f(x + kh) - f(x - kh)) \quad (2.30)$$

where $h = 1/2^n$, $x \in B_m$, $m \le n$, and

$$r_k = \int_{-\infty}^{+\infty} \varphi(x - k)\frac{d}{dx}\varphi(x)\,dx. \quad (2.31)$$

The coefficients r_k may be computed (see [2]) by solving

$$r_k = 2\left[r_{2k} + \frac{1}{2}\sum_{l=1}^{L/2} a_{2l-1}(r_{2k-2l+1} + r_{2k+2l-1})\right]$$

and

$$\sum_{k\in Z} k r_k = -1, \quad (2.32)$$

where the coefficients a_{2l-1} are given in (2.5). If the number of vanishing moments of the wavelet $M \ge 2$, then equations (2.32) have a unique solution with a finite number of nonzero r_k, namely, $r_k \ne 0$ for $-L + 2 \le k \le L - 2$ and $r_k = -r_{-k}$.

We will use the iterative interpolation scheme and the procedure for computing the derivative in Section IV to find zero-crossings of signals and the slopes at the zero-crossings.

III. Auto-Correlation Shell: A Shift-Invariant Multiresolution Representation

Let us assume that the finest scale of interest is described by the $N = 2^n$ dimensional subspace $V_0 \subset L^2(\mathbf{R})$ and consider only circulant shifts on V_0. We refer to the set of functions $\{\Psi_{j,k}(x)\}_{1\le j\le n_0, 0\le k\le N-1}$ and $\{\Phi_{n_0,k}(x)\}_{0\le k\le N-1}$ as a *shell* of the auto-correlation functions of orthonormal wavelets (an *auto-correlation shell* for short), where n_0 ($\le n$) describes the coarsest scale of interest and

$$\Phi_{j,k}(x) = 2^{-j/2}\Phi(2^{-j}(x - k)),$$

$$\Psi_{j,k}(x) = 2^{-j/2}\Psi(2^{-j}(x - k)). \quad (3.33)$$

Let us describe a fast algorithm to expand a function $f \in V_0 = \overline{\text{span}\{\varphi_{0,k};\, k \in \mathbf{Z}\}}$, $f = \sum_{k=0}^{N-1} s_k^0 \varphi_{0,k}$. Let the coefficients $\{p_k\}$ and $\{q_k\}$ be those of the two-scale difference equations (2.7) and (2.10) which we write as

$$p_k = \begin{cases} 2^{-1/2} & \text{for } k = 0, \\ 2^{-3/2}a_{|k|} & \text{otherwise,} \end{cases}$$

$$q_k = \begin{cases} 2^{-1/2} & \text{for } k = 0, \\ -p_k & \text{otherwise.} \end{cases} \quad (3.34)$$

We use these coefficients as symmetric filters $P = \{p_k\}_{-L+1\le k\le L-1}$ and $Q = \{q_k\}_{-L+1\le k\le L-1}$ with only $L/2 + 1$ distinct nonzero coefficients. Although these filters do not form a quadrature mirror filter pair, their role and use in the numerical algorithms is similar. For the shift-invariance, we now apply P and Q without subsampling at each scale, i.e.,

$$S_k^j = \sum_{l=-L+1}^{L-1} p_l S_{k+2^{j-1}l}^{j-1}, \quad (3.35)$$

$$D_k^j = \sum_{l=-L+1}^{L-1} q_l S_{k+2^{j-1}l}^{j-1}. \quad (3.36)$$

Starting from the original discrete signal $\{s_k^0\}_{0 \le k \le N-1}$, we apply (3.35) and (3.36) recursively to obtain the auto-correlation shell coefficients $\{D_k^j\}_{1 \le j \le n_0, 0 \le k \le N-1}$ and $\{S_k^{n_0}\}_{0 \le k \le N-1}$.

We obtain the following relation between the original discrete signal and the auto-correlation shell coefficients:

Proposition 1: For any function $f \in V_0$, $f(x) = \sum_{k=0}^{N-1} s_k^0 \varphi(x - k)$, the coefficients $\{S_k^j\}$ and $\{D_k^j\}$ computed via (3.35) and (3.36) satisfy the following identities

$$\sum_{k=0}^{N-1} S_k^j \Phi_{0,k} = \sum_{k=0}^{N-1} s_k^0 \Phi_{j,k}, \tag{3.37}$$

$$\sum_{k=0}^{N-1} D_k^j \Phi_{0,k} = \sum_{k=0}^{N-1} s_k^0 \Psi_{j,k} \tag{3.38}$$

where $\Phi_{j,k}$ and $\Psi_{j,k}$ are defined in (3.33).

Proof: Using the coefficients p_k in (3.34), we write $\sqrt{2}\,|m_0(\xi)|^2 = \sum_{k=-L+1}^{L-1} p_k e^{ik\xi}$. Substituting this into the Fourier transform of (3.35), we obtain

$$\hat{S}^j(\xi) = \hat{s}^0(\xi) 2^{j/2} \prod_{l=1}^{j} |m_0(2^{l-1}\xi)|^2. \tag{3.39}$$

We then take the Fourier transform of the left hand side of (3.37), use (3.39) and the identity $\hat{\Phi}(\xi) = \Pi_{l=1}^{\infty} |m_0(2^{-l}\xi)|^2$, to obtain

$$\begin{aligned} \hat{S}^j(\xi)\hat{\Phi}(\xi) &= \hat{s}^0(\xi) 2^{j/2} \prod_{l=1}^{j} |m_0(2^{l-1}\xi)|^2 \hat{\Phi}(\xi) \\ &= \hat{s}^0(\xi) 2^{j/2} \hat{\Phi}(2^j \xi) \end{aligned} \tag{3.40}$$

which is exactly (3.37) in the Fourier domain. The relation (3.38) may be derived similarly. □

This proposition plays an essential role in our approach to the reconstruction of signals from zero-crossings in Section IV.

Let us now construct an algorithm for reconstructing the original signal directly from the auto-correlation shell coefficients. Since $p_k = -q_k$ for $k \neq 0$ in (3.34), adding (3.35) and (3.36) yields a simple reconstruction formula

$$S_k^{j-1} = \frac{1}{\sqrt{2}} (S_k^j + D_k^j),$$

$$j = 1, \cdots, n_0, \quad k = 0, \cdots, N-1. \tag{3.41}$$

Given the auto-correlation shell coefficients

$$\{D_k^j\}_{1 \le j \le n_0, 0 \le k \le N-1} \quad \text{and} \quad \{S_k^{n_0}\}_{0 \le k \le N-1},$$

(3.41) leads to

$$s_k^0 = 2^{-n_0/2} S_k^{n_0} + \sum_{j=1}^{n_0} 2^{-j/2} D_k^j, \qquad k = 0, \cdots, N-1. \tag{3.42}$$

Examples of representation of signals in the auto-correlation shell are presented in Figs. 4 and 5.

Remark 1: It is easy to adjust the auto-correlation shell to "life on the interval." (See [5] for a more delicate construction for wavelets.) Since our filter coefficients p_k are obtained by evaluating the Lagrange polynomials at the origin $x = 0$ [see (2.19)], it is natural to adjust the filter coefficients for the edges by simply generating them by evaluating these polynomials at the desired points. For example, for the lowpass filter coefficients $2^{-1/2}\{-1/16, 0, 9/16, 1, 9/16, 0, -1/16\}$ based on Daubechies's QMF with $L = 2M = 4$, the adjusted lowpass filter coefficients for the left edge are $2^{-1/2}\{5/16, 1, 15/16, 0, -5/16, 0, 1/16\}$. These coefficients are convolved with the leftmost 7 points of the signal to obtain the 2nd leftmost point of the next scale.

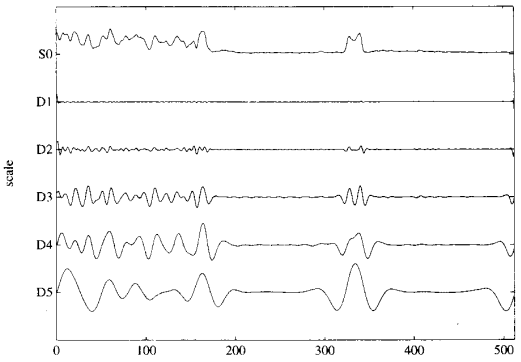

Fig. 4. The expansion of the signal in the auto-correlation shell using the auto-correlation functions of Daubechies's wavelet with $L = 2M = 4$. The top row is the original signal. Note that the locations of edges in the original signal correspond to the zero-crossings in this representation.

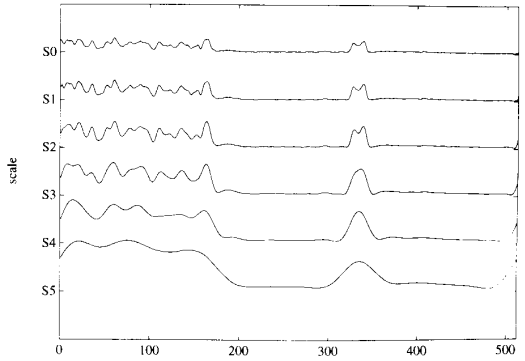

Fig. 5. The average coefficients on different scales. (The top row is the original signal).

Remark 2: Representations using the auto-correlation functions of compactly supported wavelets can also be viewed as a way to obtain a "continuous" multiresolution analysis. Another approach to make the connection between continuous and discrete multiresolution analyses is developed in [11], where the starting point is a continuous version of the multiresolution analysis.

Remark 3: Representations using the auto-correlation functions of compactly supported wavelets should be compared with those using the approximation of the Laplacian of a Gaussian function (the so-called Mexican-hat function) by the Difference of two Gaussian functions (the so-called DOG function) as

$$\frac{d^2}{dx^2} G(x; \sigma) \approx aG(ax; \sigma) - G(x; \sigma) \tag{3.43}$$

where

$$G(x; \sigma) = \frac{1}{\sqrt{2\pi}\,\sigma} e^{-x^2/2\sigma^2} \tag{3.44}$$

and $a = 1.6$ as was suggested in [17]. It follows from (2.7) and (2.10) that

$$\Psi(x) = 2\Phi(2x) - \Phi(x) \tag{3.45}$$

which should be compared with (3.43).

IV. On Reconstructing Signals from Zero-Crossings

Since the auto-correlation functions of compactly supported wavelets may be viewed as pseudo-differential operators of even order, and essentially behave like derivative operators of the same order, the zero-crossings in this representation correspond to the locations of edges at different scales in the signal. Dubuc's iterative interpolation is naturally associated with such a representation and allows us to *define* zero-crossings for multiresolution representations of *discrete* signals. By using the iterative interpolation, we locate the zero-crossings and compute slopes at these points within the prescribed numerical accuracy. To reconstruct the signal, we set up a system of linear algebraic equations, where the entries of the matrix are computed from the values of the auto-correlation function and its derivative at the integer translates of zero-crossings. The original signal is then reconstructed within the prescribed accuracy by solving this linear system.

Reconstructing a signal from its zero-crossings by solving a linear system of equations has been proposed by Curtis and Oppenheim [6]. Their method requires a solution of a linear system where the unknowns are the Fourier coefficients and, therefore, the linear system is dense. It also requires multiple threshold-crossings rather than zero-crossings, and moreover, the quality of the reconstruction strongly depends on the choice of the thresholds. We would like to note that in our approach we take advantage of the multiresolution properties of the auto-correlation shell which allows us to set the linear system directly for the unknown signal rather than the coefficients of its expansion.

Remark 4: We note that our approach may be modified to produce the maxima-based representation of Mallat and Zhong [16] by considering $\int_{-\infty}^{x} \Psi(y)\,dy$ instead of $\Psi(x)$ and the corresponding two-scale difference equation. Using the symmetric iterative interpolation, we have better numerical control than by using to the approaches developed by Mallat and Zhong [16] and by Hummel and Moniot [12].

Remark 5: We would like to emphasize that our zero-crossing-based representation is not aimed at data compression. It should be used for nonlinear manipulations of signals such as edge-preserving smoothing by retaining the zero-crossings whose slopes are significant (see [15]).

Let us now describe our procedure for the zero-crossing computation. Using the symmetric iterative interpolation scheme mentioned above, we compute the zero-crossing locations of the set of functions $\{\Sigma_{k=0}^{N-1} D_k^j \Phi(x-k)\}_{1 \le j \le n_0}$ within the prescribed numerical accuracy, e.g., $\epsilon = 10^{-14}$. To compute the location of a zero-crossing, we recursively subdivide the unit interval bracketing the zero-crossing until the length of the subdivided interval bracketing that zero-crossing becomes less than the accuracy ϵ. The iterative interpolation scheme allows us to zoom in as much as we want around the zero-crossing. This process requires at most $O(-L \log_2 \epsilon)$ operations per zero-crossing. Once the zero-crossing is found, the computation of the slope is merely the convolution of the $2(L-2)$ points around the zero-crossing with the filter coefficients $\{r_l\}_{-L+2 \le l \le L-2}$ in (2.30).

We now address the following problem: Given the coarsest subsampled coefficients $\{S_{2^{n_0}k}^{n_0}\}_{0 \le k \le 2^{N-n_0}-1}$ and the zero-crossings and the slopes at these zero-crossings $\{x_m^j, v_m^j\}_{1 \le j \le n_0, 0 \le m \le N_z^j - 1}$, where N_z^j is the number of zero-crossings of the function $\Sigma_{k=0}^{N-1} D_k^j \Phi(x-k)$, reconstruct the original vector $\{s_k^0\}_{0 \le k \le N-1}$. Proposition 1 provides a simple mechanism for defining a linear system which relates the unknown signal $\{s_k^0\}$ and the values of the function $\Phi(x)$ and its derivative at the integer translates of zero-crossings.

It follows from Proposition 1, that any zero-crossing coordinate x_m^j satisfies

$$\sum_{k=0}^{N-1} D_k^j \Phi(x_m^j - k) = \sum_{k=0}^{N-1} s_k^0 \Psi_{j,k}(x_m^j) = 0, \tag{4.46}$$

$$\sum_{k=0}^{N-1} D_k^j \Phi'(x_m^j - k) = \sum_{k=0}^{N-1} s_k^0 2^{-j} \Psi'_{j,k}(x_m^j) = v_m^j \tag{4.47}$$

where $1 \le j \le n_0$, $0 \le m \le N_z^j - 1$. Similarly, we have

$$\sum_{k=0}^{N-1} S_k^{n_0} \Phi_{0,k}(2^{n_0} l) = \sum_{k=0}^{N-1} s_k^0 \Phi_{n_0,k}(2^{n_0} l) = S_{2^{n_0} l}^{n_0} \tag{4.48}$$

for $l = 0, 1, \cdots, N_s - 1$, where $N_s = 2^{n-n_0}$.

We rewrite (4.46), (4.47), and (4.48) in a vector-matrix form as

$$\boldsymbol{A}\boldsymbol{s} = \boldsymbol{v} \tag{4.49}$$

where $\boldsymbol{s} \in \boldsymbol{R}^N$ is a shorthand notation for the original signal $\{s_k^0\}$, $\boldsymbol{v} \in \boldsymbol{R}^{2N_z + N_s}$ is a data vector including the slopes and available coarsest subsampled coefficients, i.e.,

$$\boldsymbol{v} = (0, v_0^1, \cdots, 0, v_{N_z^1 - 1}^1, \cdots, 0, v_0^{n_0}, \cdots 0, \quad v_{N_z^{n_0}-1}^{n_0},$$
$$S_0^{n_0}, S_{2^{n_0}}^{n_0}, \cdots, S_{N-2^{n_0}}^{n_0})^T \tag{4.50}$$

and $\boldsymbol{A}$ is a $(2N_z + N_s) \times N$ matrix and has the following structure:

$$\boldsymbol{A} = \begin{pmatrix} \boldsymbol{A}^1 \\ \boldsymbol{A}^2 \\ \vdots \\ \boldsymbol{A}^{n_0} \\ \boldsymbol{S}^{n_0} \end{pmatrix} \tag{4.51}$$

and $\boldsymbol{A}^j$ is a $2N_z^j \times N$ submatrix whose entries are

$$(\boldsymbol{A}^j)_{2k,l} = \Psi_{j,l}(x_k^j), \qquad (\boldsymbol{A}^j)_{2k+1,l} = 2^{-j} \Psi'_{j,l}(x_k^j),$$
$$k = 0, \cdots, N_z^j - 1, \qquad l = 0, \cdots, N-1 \tag{4.52}$$

and $\boldsymbol{S}^{n_0}$ is a $N_s \times N$ submatrix where

$$(\boldsymbol{S}^{n_0})_{k,l} = \Phi_{n_0,l}(2^{n_0} k), \qquad k = 0, \cdots, N_s,$$
$$l = 0, \cdots, N-1. \tag{4.53}$$

Since the auto-correlation function $\Psi_{j,k}(x)$ is compactly supported, the matrix $\boldsymbol{A}$ is sparse by construction. It is easy to check that the support of the function $\Psi_{j,k}(x)$ is $2^{j+1}(L-1)$. Thus, the number of N_A of nonzero entries of the matrix $\boldsymbol{A}$ is as follows:

$$N_A = \sum_{j=1}^{n_0} 2N_z^j 2^{j+1}(L-1) + N_s 2^{n_0+1}(L-1)$$
$$= 2(L-1)\left[\sum_{j=1}^{n_0} 2^j 2N_z^j + N\right]. \tag{4.54}$$

The number of zero-crossings usually decreases as the scale j increases. As a result, the number of the nonzero entries of the matrix $\boldsymbol{A}$ is essentially $O(N)$. The sparsity of this matrix enables one to solve the system (4.49) efficiently.

Whether we can solve the linear system (4.49) depends on the condition number of the matrix (4.51), which is affected by the distribution of locations of zero-crossings. If there are very few zero-crossings (which means that the signal is zero over a significant part of its support) as, for example, in the expansion of the unit impulse $\{s_k^0 = \delta_{k_0,k}\}$ with only $2L$ zero-crossings at each scale, then we need to use additional constraints for solving the linear system (4.49). There might be several approaches to introduce these additional constraints. One approach (which might be sufficient in some applications) would be to consider the generalized inverse of (4.51). Another possible approach (that we have expermented with) is to introduce a heuristic constraint that the distance between the adjacent zero-crossings at the jth scale does not exceed $2^{j+1}(L-1)$. The latter constraints may be expressed as

$$\boldsymbol{C}\boldsymbol{d} = \boldsymbol{0}. \tag{4.55}$$

where $\boldsymbol{d} \in \boldsymbol{R}^{Nn_0 + N_s}$ is a vector of auto-correlation shell coefficients including the subsampled coarsest averages, i.e.,

$$\boldsymbol{d} = (D_0^1, \cdots, D_{N-1}^1, \cdots, D_0^{n_0}, \cdots, D_{N-1}^{n_0}, S_0^{n_0}, S_{2^{n_0}}^{n_0}, \cdots, S_{N-2^{n_0}}^{n_0})^T, \tag{4.56}$$

and $\boldsymbol{C}$ is an $(Nn_0 + N_s)$ dimensional square matrix of the form

$$\begin{pmatrix} \boldsymbol{C}^1 & \boldsymbol{0} & \cdots & \cdots & \boldsymbol{0} \\ \boldsymbol{0} & \boldsymbol{C}^2 & \cdots & \cdots & \vdots \\ \vdots & & \ddots & & \vdots \\ \vdots & & & \ddots & \vdots \\ \boldsymbol{0} & \cdots & \cdots & \boldsymbol{C}^{n_0} & \boldsymbol{0} \end{pmatrix} \tag{4.57}$$

where the submatrix $\boldsymbol{C}^j$ is an N dimensional diagonal matrix as

$$(\boldsymbol{C}^j)_{k,k} = \begin{cases} 1 & \text{if } D_k^j \text{ must be zero,} \\ 0 & \text{otherwise.} \end{cases} \tag{4.58}$$

(4.55) may be expressed in terms of the original signal $\boldsymbol{s}$ by using the transformation matrix $\boldsymbol{T} \in \boldsymbol{R}^{(Nn_0 + N_s) \times N}$ from $\boldsymbol{s}$ to $\boldsymbol{d}$:

$$\boldsymbol{C}\boldsymbol{d} = \boldsymbol{B}\boldsymbol{s} = \boldsymbol{0}, \tag{4.59}$$

where $\boldsymbol{B} \in \boldsymbol{R}^{(Nn_0 + N_s) \times N}$ and $\boldsymbol{B} = \boldsymbol{C}\boldsymbol{T}$.

The problem may now be stated as follows:

$$\text{Minimize } \|\boldsymbol{A}\boldsymbol{s} - \boldsymbol{v}\| \text{ subject to } \boldsymbol{B}\boldsymbol{s} = \boldsymbol{0}. \tag{4.60}$$

Using the method of Lagrange multipliers, we obtain the least square solution

$$\hat{\boldsymbol{s}} = (\boldsymbol{A}^T\boldsymbol{A} + \lambda \boldsymbol{B}^T\boldsymbol{B})^{-1}\boldsymbol{A}^T\boldsymbol{v}. \tag{4.61}$$

We note that our formulation is completely linear except for the process of zero-crossing detection. It is clear from (4.49) and (4.60), that the slope information is essential for signal reconstruction since if there is no slope information, we have only the trivial solution, $\boldsymbol{s} = \boldsymbol{0}$. Previously, this fact was examined only empirically [12].

Let us show two examples of the reconstruction using our method. The accuracy threshold ϵ has been set to 10^{-14} in both cases. As a first example, we have used the signal shown in Fig. 4 in Section III. The relative L^2 error of the reconstructed signal compared with the original signal is $\approx 5.7 \times 10^{-13}$. In this case, there was no need to use the constraints.

Next we have applied our algorithm to the unit impulse $\{\delta_{32,k}\}_{0 \le k \le 63}$. Now the constraints described above play an important role: the relative L^2 error with the constraints is $\approx 7.4 \times 10^{-15}$ whereas the error of the solution using the generalized inverse without the constraints is $\approx 3.2 \times 10^{-4}$.

References

[1] R. Ansari, C. Guillemot, and J. F. Kaiser, "Wavelet construction using Lagrange halfband filters," *IEEE Trans. Circuits Syst.*, vol. 38, pp. 1116–1118, Sept. 1991.

[2] G. Beylkin, "On the representation of operators in bases of compactly supported wavelets," *SIAM J. Numer. Anal.*, vol. 29, pp. 1716–1740, Dec. 1992.

[3] P. J. Burt, "Fast filter transforms for image processing," *Comput. Graphics, Image Processing*, vol. 16, pp.20–51, 1981.

[4] A. Cohen, I. Daubechies, and J.-C. Feauveau, "Biorthogonal bases of compactly supported wavelets," *Commun. Pure Appl. Math.*, vol. 45, pp. 485–560, June 1992.

[5] A. Cohen, I. Daubechies, B. Jawerth, and P. Vial, "Multiresolution analysis, wavelets, and fast algorithms on an interval," *Comptes Rendus Acad. Sci. Paris (A)*, 1992, Série I, vol. 316, pp. 417–421, Mar. 1993.

[6] S. R. Curtis and A. V. Oppenheim, "Reconstruction of multidimensional signals from zero crossings," *J. Opt. Soc. Amer.*, vol. 4, pp.221–231, Jan. 1987.

[7] J. Daubechies, "Orthonormal bases of compactly supported wavelets," *Commun. Pure Appl. Math.*, vol. 41, pp. 909–996, 1988.

[8] ——, "Orthonormal bases of compactly supported wavelets II. Variations on a theme," *SIAM J. Math. Anal.*, vol. 24, pp. 499–519, Mar. 1993.

[9] G. Deslauriers and S. Dubuc, "Symmetric iterative interpolation processes," *Constr. Approx.*, vol. 5, pp. 49–68, 1989.

[10] S. Dubuc, "Interpolation through an iterative scheme," *J. Math. Anal. Appl.*, vol. 114, pp. 185–204, 1986.

[11] M. Duval-Destin, M. A. Muschietti, and B. Torresani, "Continuous wavelet decompositions, multiresolution and contrast analysis," *SIAM J. Math. Anal.*, vol. 24, pp. 739–755, May 1993.

[12] R. Hummel and R. Moniot, "Reconstruction from zero crossings in scale space," *IEEE Trans. Acoust., Speech, Signal Processing*, vol. 37, pp. 2111–2130, Dec. 1989.

[13] R. Kronland-Martinet, J. Morlet, and A. Grossmann, "Analysis of sound patterns through wavelet transforms," *J. Pattern Recognition, Artificial Intell.*, vol. 1, no. 2, pp. 273–302, 1987.

[14] S. Mallat, "A theory for multiresolution signal decomposition," *IEEE Trans. Patt. Anal. Mach. Intell.*, vol. 11, pp. 674–693, July 1989.

[15] S. Mallat and W. L. Hwang, "Singularity detection and processing with wavelets," *IEEE Trans. Informat. Theory*, vol. 38, pp. 617–643, Mar. 1992.

[16] S. Mallat and S. Zhong, "Characterization of signals from multiscale edges," *IEEE Trans. Patt. Anal. Mach. Intell.*, vol. 14, pp. 710–732, July 1992.

[17] D. Marr, *Vision*. San Francisco: Freeman, 1982.

[18] S. Osher and L. I. Rudin, "Feature-oriented image enhancement using shock filters," *SIAM J. Numer. Anal.*, vol. 27, pp. 919–940, Aug. 1990.

[19] P. Perona and J. Malik, "Scale-space and edge detection using anisotropic diffusion," *IEEE Trans. Patt. Anal. Mach. Intell.*, vol. 12, pp. 629–639, July 1990.

[20] O. Rioul and P. Duhamel, "Fast algorithms for discrete and continuous wavelet transforms," *IEEE Trans. Informat. Theory*, vol. 38, pp. 569–586, Mar. 1992.

[21] N. Saito and G. Beylkin, "Multiresolution representations using the auto-correlation functions of compactly supported wavelets," Schlumberger-Doll Research, Ridgefield, CT, Tech. Rep., Aug. 1991. Expanded abstract in *Proc. ICASSP-92*, vol. 4, Mar. 1992, pp. 381–384.

[22] M. J. Shensa, "The discrete wavelet transform: Wedding the à trous and Mallat algorithms," *IEEE Trans. Signal Processing*, vol. 40, pp. 2464–2482, Oct. 1992.

[23] M. Vetterli and C. Herley, "Wavelets and filter banks: Theory and design," *IEEE Trans. Signal Processing*, vol. 40, pp. 2207–2232, Sept. 1992.